

A Fundamental Test of the Nature of Dark Matter

R. Benton Metcalf & Joseph Silk

*Departments of Physics and Astronomy, and Center for Particle Astrophysics
University of California, Berkeley, California 94720*

ABSTRACT

Dark matter may consist of weakly interacting elementary particles or of macroscopic compact objects. We show that the statistics of the gravitational lensing of high redshift supernovae strongly discriminate between these two classes of dark matter candidates. We develop a method of calculating the magnification distribution of supernovae, which can be interpreted in terms of the properties of the lensing objects. With simulated data we show that $\gtrsim 50$ well measured type Ia supernovae ($\Delta m \sim 0.16$ mag) at redshifts ~ 1 can clearly distinguish macroscopic from microscopic dark matter.

1. Introduction

The nature of dark matter (DM) poses one of the most outstanding problems in astrophysics. There are essentially two alternative hypotheses. The dark matter may be microscopic, consisting of weakly interacting particles (WIMPs) such as SUSY neutralinos or axions, or else be macroscopic, consisting of compact baryonic objects, such as primordial black holes, brown dwarfs or old white dwarfs (MACHOs). WIMPs are well-motivated but not yet detected, whereas MACHO candidates exist, but cosmological motivation is weak. However, not only do primordial black holes serve perfectly well as a cold dark matter candidate of arbitrary density, but the indications from primordial nucleosynthesis and Lyman alpha forest modeling demonstrate the necessity for a dark baryonic component of the universe. This component is plausibly MACHO-like given that the only experimental claims of DM detection are via gravitational microlensing of stars in the LMC. Of course a combination of the two types of dark matter is possible.

We propose a simple test for distinguishing macroscopic from microscopic dark matter. For simplicity we consider the opposing hypotheses that one or the other dominates. If the DM is microscopic, the clustered component, in halos, lenses high redshift supernovae (SNe). If the DM is macroscopic, most light beams do not intersect any matter - no Ricci focusing - and the SN brightness distribution is skewed to an extent that can be quantitatively distinguished from halo lensing. Current data on SNIa extend to $z = 0.97$, with most of the ~ 100 observed at $z < 0.5$. The intrinsic variance of their corrected peak luminosity in V and B band has been measured to be $\Delta M_{V,B} \simeq 0.12$ mag (Riess, Press & Kirshner 1996). High redshift type Ia SNe have already been used to put unprecedented constraints on cosmological parameters (Perlmutter *et al.* 1997, Perlmutter *et al.* 1998, Garnavich *et al.* 1998, Riess *et al.* 1998).

In §2 a method for calculating the magnification distribution function for a single lens (§2.1) and for multiple lenses (§2.2) is described. In §3 the problem of distinguishing DM candidates is addressed.

2. Properties of the Magnification Probability Distribution Function

In this paper we consider the lensing of a supernova to be done by a number of “lensing objects” or “lenses”. A lens is the smallest unit of mass that acts coherently for the purposes lensing. This could be a galaxy halo or it could be a high mass dark matter candidate such as a brown dwarf or black hole.

We make the distinction between macroscopic and microscopic DM more quantitative by considering two mass scales. The first is defined by the requirement that the projected density be smooth on the scale

of the angular size of the source. This gives a mass of

$$m_s \sim 6 \times 10^{10} \text{g} \left(\frac{\lambda_s}{\text{AU}} \right)^3 \Omega_o h^2 f \quad (1)$$

where λ_s is the physical size of the source and f is a dimensionless number of order unity. If the unit of DM is smaller then this it is microscopic DM. Another, larger mass scale is defined by the requirement that the angular size of the source be small compared to the Einstein ring radius so that it can be considered a true point source

$$m_p \sim 5 \times 10^{-7} \text{M}_\odot \left(\frac{10^3 \text{Mpc}}{D_s} \right) \left(\frac{\lambda_s}{\text{AU}} \right)^2 f \quad (2)$$

where D_s is the angular size distance to the source. If a lens is much below this mass the high magnification tail of the distribution function will be suppressed and the rare high magnification events will become time-dependent. The measured velocity of the photosphere of a type Ia SN is around $1.0 - 1.4 \times 10^4 \text{ km s}^{-1}$ which means $\lambda_s \sim 40 - 57 \Delta t \text{ AU/week}$. The SN reaches maximum light in about a week.

It is often convenient to work with the deviation of the magnification from unity denoted by $\delta\mu \equiv \mu - 1$, rather than the magnification itself μ . The background cosmology will be taken to be the standard Friedman-Lemaître-Robertson-Walker (FLRW) model described on average by the metric $ds^2 = dt^2 + a(t)^2 (d\chi^2 + D(\chi)^2 d\Omega)$ where the comoving angular size distance is $D(\chi) = \{R \sinh(\chi/R), \chi, R \sin(\chi/R)\}$ for the open, flat and closed global geometries respectively. The curvature scale is $R = |H_o \sqrt{1 - \Omega_o - \Omega_\Lambda}|^{-1}$. Another angular size distance of relevance is the Dyer-Roeder or empty-beam angular size distance, $\tilde{D}(\chi)$ (Dyer & Roeder 1974, Kantowski (1998), note difference in notation). If a bundle of light rays that converge on the observer have travel through empty space without experiencing any shear from the surrounding matter the comoving width of the bundle is $\tilde{D}(\chi)$ times its observed angular size.

2.1. Magnification by a single lens

Consider a single lens at a fixed coordinate distance from Earth. The path of the light is described by either of two lensing equations:

$$\mathbf{r}_\perp = \mathbf{y} - \alpha(\mathbf{y}, \tilde{D}_l, \tilde{D}_s) \quad (3)$$

$$\mathbf{r}_\perp = [1 - \kappa_b(\chi_s)]\mathbf{y} - \alpha(\mathbf{y}, D_l, D_s) \quad (4)$$

where \mathbf{r}_\perp is the positions of the lens relative to the undeflected line of sight to the source and \mathbf{y} is the position of its image in the same plane. The displacement between the two is

$$\alpha(\mathbf{y}_\perp, D_l, D_s) = \frac{1}{\pi} \int d^2 y' \kappa(\mathbf{y}', D_l, D_s) \frac{\mathbf{y} - \mathbf{y}'}{|\mathbf{y} - \mathbf{y}'|^2}. \quad (5)$$

where, $\kappa(\mathbf{y}, D_l, D_s)$, is the surface density expressed in units of the critical density $\Sigma_c = [4\pi G a_l D_l D_{ls} / D_s]^{-1}$. The angular size distances between the observer and the lens, the observer and the source and the lens and the source are D_l , D_s and D_{ls} respectively.

In equation (3) a negative background convergence, κ_b , is included to account for the lack of background mass density that is assumed when D is used instead of \tilde{D} . Incorporating κ_b directly into the lensing equation in this way is equivalent to the method used in Schneider, Ehlers & Falco (1992) to treat multiple scatterings in a cosmological context.

Two magnifications, $\tilde{\mu}$ and μ , can be defined using equations (3) and (4) respectively. The magnification is defined by $\mu^{-1} = \det[\partial r_i / \partial y_j]$. An expression for $\kappa_b(\chi)$ can be found by considering an object that is not lensed. The requirement that the two lensing equations agree on the true size of the object results in $\tilde{D}(\chi) = [1 - \kappa_b(\chi)]D(\chi)$. The explicit form of $\kappa_b(z)$ can be found by comparing the standard FLRW expression for $D(\chi)$ with the solutions for $\tilde{D}(\chi)$ found in Kantowski (1998). As will be mentioned in § 2.2, $\kappa_b(z)$ can also be found numerically and compared with this explicit value as a test of the numerical method.

The probability that the lens is located between r_\perp and $r_\perp + dr_\perp$ is $p(r_\perp)dr_\perp \propto r_\perp dr_\perp$. If the lens is spherically symmetric and the magnification is a monotonic function of r_\perp the expression for the magnification can be inverted (at least numerically) to get $r_\perp(\mu, D, D_s)$. The probability of a lens causing the magnification $\delta\mu$ can be found by changing variables. If the contributions from all D are included along with the possibility that the lenses are not all identical the result is

$$p(\delta\tilde{\mu})d\delta\tilde{\mu} \propto d\delta\tilde{\mu} \int \prod_i dp_i \int_0^{D_s} d\chi a(\chi) \eta(\chi, \{p\}) \\ r_\perp(\delta\tilde{\mu}, D, \{p\}) \left| \frac{\partial r_\perp(\delta\tilde{\mu}, D, \{p\})}{\partial \delta\tilde{\mu}} \right| \quad (6)$$

where $\eta(\chi, \{p\})$ is the differential number density of lenses with the set of parameters $\{p\}$. The set of parameters $\{p\}$ could include properties like mass, scale length, etc.

2.1.1. Point mass lenses

For the case of a point mass lens the total magnification of both images is given by

$$\tilde{\mu} = \frac{\hat{r}^2 + 2}{\hat{r}\sqrt{\hat{r}^2 + 4}} \quad ; \quad \hat{r} \equiv r_\perp/R_e(m, D, D_s) \quad (7)$$

where R_e is the Einstein radius of the lens, $R_e^2 = 4Gm\tilde{D}_l\tilde{D}_{ls}/\tilde{D}_s$. Equation (7) can be inverted and with equation (6) the one lens distribution function is

$$p(\delta\tilde{\mu})d\delta\tilde{\mu} \propto [(1 + \delta\tilde{\mu})^2 - 1]^{-3/2} d\delta\tilde{\mu}. \quad (8)$$

The probability in (8) is not normalizable; it diverges at small $\delta\tilde{\mu}$. This is a generic feature which is due to the fact that at infinite radii there are an infinite number of positions for the lenses. This can be handled by introducing a cutoff in either $\delta\tilde{\mu}$ space or in r_\perp . The nature of this cutoff is not important as long as it is at sufficiently small $\delta\tilde{\mu}$ or large r_\perp . This will be clear when the total magnification distribution due to multiple lenses is considered.

Another generic feature of one-lens distribution functions that is present in (8) is that unless an inner cutoff is introduced some moments are infinite. In the point mass case $p(\delta\tilde{\mu}) \sim \delta\tilde{\mu}^{-3}$ for $\delta\tilde{\mu} \gg 1$ so the second and higher moments diverge. Lens models typically have power law mass density distributions near their center and will thus also have divergent moments. One manifestation of this is that experimental estimates of the moments such as the mean and variance will converge slowly if at all. This is something that should be kept in mind when constructing statistical estimators.

2.1.2. Halo lenses

If the dark matter consists of microscopic particles clumped into halos, the entire halo will act as a single lens. In this case the Ricci focusing contribution to the magnification strongly dominates over shear

distortions produced by mass outside of the beam (Holz & Wald 1998, Premadi, Martel & Matzner 1998). The magnification is then a function of only the local dimensionless surface density, $\kappa(\mathbf{y})$. Furthermore the lensing of the great majority of SNe will be quite weak which allows us to confidently make the linear approximation: $\delta\mu = 2[\kappa(\mathbf{y}, D_l, D_s) + \kappa_b]$. This assumption has been well justified by many authors and will be confirmed by results in §2.2. Equation (6) can then be used with r_\perp replaced with y_\perp and an additional factor of $(1 + \kappa)^{-1}$ to account for the images not being uniformly distributed - lenses are uniformly distributed in \mathbf{r}_\perp -space.

For the purposes of this paper it will suffice to use a simple model for the surface density of halos. We use models with surface densities given by

$$\Sigma(y_\perp) = \frac{V_c^2}{2Gy_\perp} \left[\left(\frac{y_\perp}{r_s} \right)^2 + 1 \right]^{-1} \quad (9)$$

This model behaves like a singular isothermal sphere out to $y_\perp \simeq r_s$ where it is smoothly cut off. Expression (9) can be analytically inverted to get $\kappa(y_\perp)$.

In the following calculations, each halo is assumed to harbor a galaxy. At all redshifts a Schechter luminosity function fit to local galaxies is assumed with $\alpha = -1.07$ and $\phi^* = 0.01(1 + z)^3h^3 \text{ Mpc}^{-3}$. The luminosities are then related to the circular velocity, V_c , by the local Tully-Fisher relation, $V_c = V_*(L/L_*)^{0.22}$ where $V_* = 200 \text{ km s}^{-1}$ will be used. The scale lengths are related to the luminosity through $r_c = r_*(L/L_*)^{1/2}$ with $r_* = 220 \text{ kpc}$. The precise values used for these parameters do not have a significant effect on the results of this paper.

2.2. Total Magnification

The total magnification of a source includes contributions from all the lenses surrounding the light path. To find the true path connecting a source to us the lensing equation must be solved with multiple deflections (see Schneider, Ehlers & Falco (1992)). The magnifications due to different lens planes are in general nonlinearly coupled. However, if the deflections due to no more than one of the lenses is very weak the coupling between lenses can be ignored and their magnifications, $\delta\mu$ or $\delta\tilde{\mu}$, will add linearly. This is a good approximation for the vast majority of light paths in realistic models. The validity of this assumption will be justified by the results and is further investigated in Metcalf (1999). Furthermore numerical simulations and analytic arguments show that for both kinds of DM it is a good approximation to take the lenses to be uncorrelated in space (see Holz & Wald 1998, Metcalf (1998b)). This is because the probability of multiple significant deflections within a correlated region of space is very small. If in addition we take the lenses internal properties to be uncorrelated, the probability that the total magnification, $\delta\tilde{\mu}_s$, of a point source is between $\delta\tilde{\mu}_s$ and $\delta\tilde{\mu}_s + d\delta\tilde{\mu}_s$ is

$$P(\delta\tilde{\mu}_s)d\delta\tilde{\mu}_s = d\delta\tilde{\mu}_s \int \prod_{i=1}^N [d\delta\tilde{\mu}_i p(\delta\tilde{\mu}_i)] \delta(\delta\tilde{\mu}_s - \sum_{i=1}^N \delta\tilde{\mu}_i) \quad (10)$$

where the $\delta\tilde{\mu}_i$ is the contribution of the i th lens.

The magnification $\delta\mu_s$ is defined as the deviation of the luminosity from its mean value. As a result, the mean of the distribution $P(\delta\mu_s)$ must vanish.¹ This combined with the requirement that both

¹The actual mean angular size distance should be slightly larger than the FLRW value because galaxies obscure some sources.

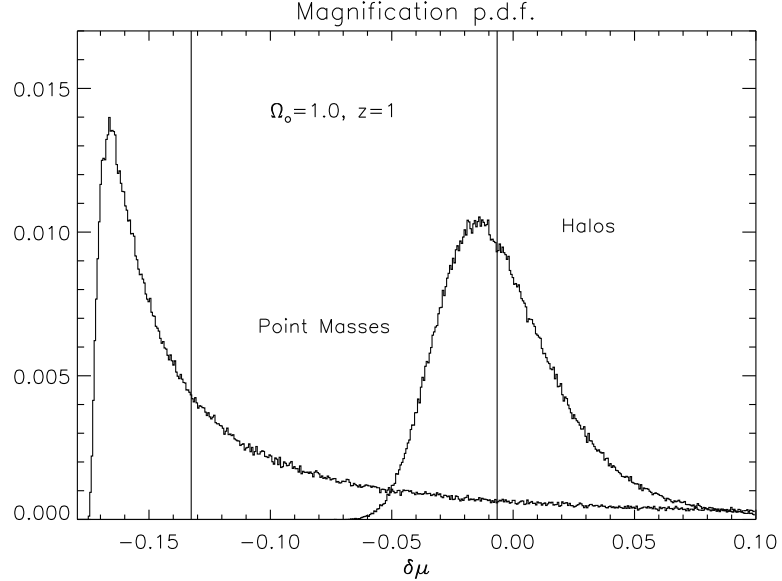


Fig. 1.— These are histograms representing the total magnification probability distribution for macroscopic DM and microscopic DM clumped into halos. The mean of both distributions is zero. The vertical lines mark the medians. For the macroscopic DM case all the matter in the universe is in the lenses. The DM halos have a total mass of $\Omega_h = 0.8$.

magnifications agree on the true size of a source results in the expression $1 - \kappa_b(\chi) = \langle \tilde{\mu}(\chi) \rangle^{1/2}$. In this way the value of $\kappa_b(\chi)$ can be found by calculating the mean of (10) numerically and a check can be made by comparing the results with the explicit values for $D(\chi)$ and $\tilde{D}(\chi)$. These values agree to a few percent which is consistent with the uncertainty introduced by the discrete nature of the numerical calculation in the power law tail of the distribution. If all the matter in the universe is not within the lenses - there is a smoothly distributed component - $\kappa_b(\chi)$ calculated in this way will be larger (closer to zero). For this reason the $\kappa_b(\chi)$ calculated in a microscopic DM model may not agree with the one for a macroscopic DM model. To compare the two, one of the distribution functions should be shifted so that they have the same mean.

As the number of lenses, N , increases the shape of the distribution (10) converges. If a cutoff is put into the halo model, N is determined by the number density of halos. The number of point mass lenses is set by the $\delta\mu_{min}$ assumed. If $\delta\mu_{min}$ is set small enough the mass outside the volume defined by $r_\perp(\delta\mu_{min})$ can be considered to be uniformly distributed for the purposes of lensing.

Figure 1 shows two examples of histograms made by producing random values $\delta\tilde{\mu}_i$ drawn from the single lens distributions and then adding them to get the total magnification. The point mass or macroscopic DM distribution shown in figure 1 peaks well below its mean and near the empty-beam solution which is $\delta\mu = -0.21$ in this case. This is because in this case most lines of sight do not come very close to any lens. There is a large high magnification tail which is of precisely the same form as the one lens distribution function, (8), right up to the peak. The probability that there are two lenses which individually give magnifications greater than $\delta\mu$ becomes appreciable only below this peak. This supports our approximation that whenever the lensing is strong it is dominated by one lens and there is no coupling between lenses.

Galaxies are presumably correlated with high density regions through which the magnification would be above average were they transparent.

In addition we have compared our results with the numerical simulations of Holz & Wald 1998 and found excellent agreement.

At low enough magnification it becomes improbable that there is not a lens close enough to the line of sight to produce that much magnification. The position of the peak can be estimated by the magnification for which the optical depth approaches one. In the microscopic DM case this happens at a higher magnification and there are no lines of sight extending to high redshift which are “empty”, i.e. $\delta\tilde{\mu} = 0$. The high magnification tail is also suppressed because of the relative rarity of halo cores which are, in any case, likely to be highly extincted. The widths of the peaks are related to the rate at which the magnification falls off with distance from the lens. The macroscopic DM magnification distribution is independent of the mass of the lenses, depending only on the total mass density in lenses and the redshift of the source.

3. Distinguishing Dark Matter Candidates

The apparent luminosity of a SN, l , after lensing can be expressed in terms of either of the two magnifications

$$l = \mu \langle l \rangle = \frac{\tilde{\mu}}{\langle \tilde{\mu} \rangle} \langle l \rangle. \quad (11)$$

We wish to infer with the measured luminosities of a set of SNe, each located at a different redshift, from which distribution the magnifications were drawn and in this way surmise which DM candidate is most likely. To establish some insight into the magnitude of this effect, the difference in magnitudes between the average and the empty-beam solutions at $z = 1$ are: -0.25 mag for $\Omega_o = 1$, -0.14 mag for flat $\Omega_o = 0.3$ and -0.10 mag for open $\Omega_o = 0.3$.

To model the results of observations we must of course add noise to the two trial distribution functions. This noise originates from both the intrinsic distribution of SN luminosities and the observational noise. Here we will model the noise as Gaussian-distributed in magnitude with a standard deviation of 0.16 mag. The noise will then be lognormally distributed in $\delta\mu$ which gives it a long tail that to some extent mocks the effects of lensing. If the noise is assumed to be Gaussian in luminosity, significantly stronger constraints can be made.

Let us denote the probability of getting a data set, $\{\delta\mu\}$, given a model - either microscopic or macroscopic DM - as $P(\{\delta\mu\}|model) = \prod_i P(\delta\mu_i|model)d\delta\mu_i$ where the product is over the observed SNe. This can be calculated numerically from the probability distributions discussed in §2.2. Because of Bayes’ theorem we know that the ratio of these two probabilities is equal to the relative likelihood of the models being correct, the odds, given a data set. It is more convenient to work with the statistic

$$\mathcal{M}_p \equiv \frac{1}{N_{SN}} \ln \left[\frac{P(\{\delta\mu\} | \text{ particles})}{P(\{\delta\mu\} | \text{ halos})} \right]. \quad (12)$$

For a modest number of SNe, N_{SN} , this statistic has the advantage of being very close to Gaussian distributed despite the power law tail in the magnification distribution function. The mean of the \mathcal{M}_p is a direct prediction of the model, independent of N_{SN} .

Figure 2 shows how much the distributions of \mathcal{M}_p with macroscopic DM and microscopic DM overlap. The cumulative probabilities are plotted integrating from left to right in the case of macroscopic DM and from right to left in the case of microscopic DM. A measure of the ability of this statistic to discriminate between models is the height of the point where the two curves with the same number of SNe cross. For example if $\Omega_o = 1$ and 21 SNe are observed at $z \sim 1.0$ about 95% of the time one of the models will be ruled out (relative to the other) at *better* than 95% confidence. For fixed Ω_o , models with $\Omega_\Lambda = 0$ have the

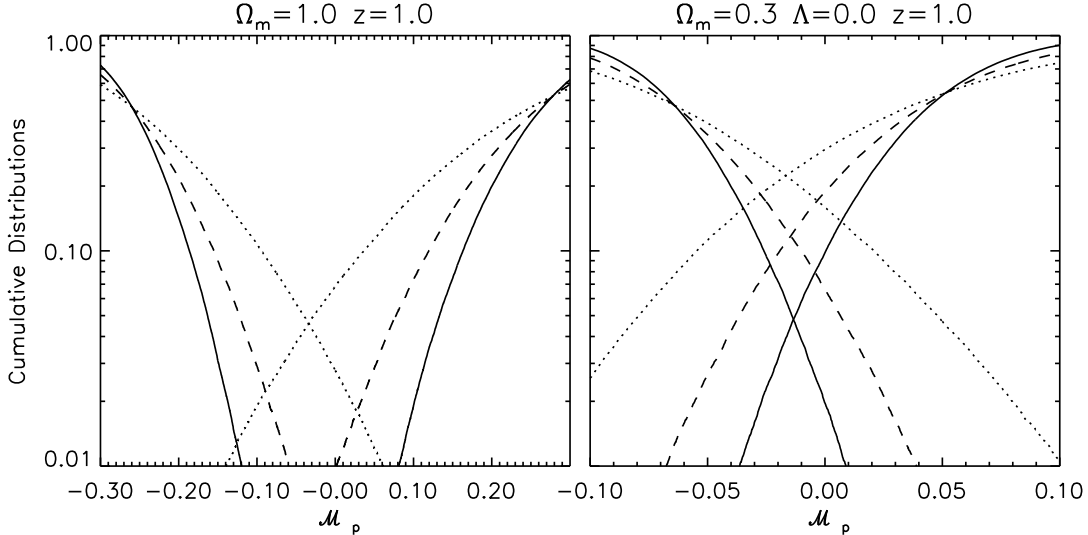


Fig. 2.— Differentiating dark matter candidates: These are the cumulative distributions of the statistic \mathcal{M}_p for data sets containing 21 (dotted), 51 (dashed) and 101 (solid) SNe at $z = 1$. The curves rising toward the left are for the case of clustered microscopic DM. The curves rising toward the right are for macroscopic DM. The right panel is for $\Omega_o = 1.0$ and the halos have total density $\Omega_h = 0.8$. The left panel is for $\Omega_o = 0.3$ and $\Omega_\Lambda = 0.0$ with the halo model having $\Omega_h = 0.27$.

least ability to differentiate the DM candidates, but even in this case, as figure 2 shows, with 51 SNe at the same redshift and $\Omega_o = 0.3$ we expect to get better than 89% confidence 89% of the time.

The mean luminosity, $\delta\mu = 0$, of a SN at a given redshift is fixed by observations of low redshift SNe and the background cosmology. The background cosmology could be simply assumed or it could be determined simultaneously from the SN sample. SNe at $z \sim 0.5$ will not be strongly affected by lensing, but can be used for cosmological parameter estimation. In figure (2) we have assumed that the mean luminosity is already fixed by lower redshift SNe. This is not necessary, but is reasonable given that the sample of lower redshift SNe will probably always be significantly larger than the sample at $z \sim 1$. Using only the $z \sim 1$ sample to simultaneously fix the cosmology and the lensing only slightly weakens the ability of \mathcal{M}_p to discriminate. The power of lensing to differentiate DM candidates comes mostly from its ability to identify macroscopic DM. A positive detection of the lensing by microscopic DM halos will take more SNe unless the correlations between SN luminosities and observed galaxies are utilized (Metcalf (1998b), Metcalf (1999)).

4. Discussion

One concern in implementing the test described here is the possibility that type Ia SNe and/or their galactic environments evolve with redshift. This is also a major concern in cosmological parameter estimation from SNe. So far there is no indication that the colors or spectra systematically change with redshift (Perlmutter *et al.* 1997, Riess *et al.* 1998). The worst case scenario would be that the luminosity distribution of type Ia SNe has a long high luminosity tail that increases with redshift. Since the evolution of the magnification distribution is determined by cosmology it is in principle possible to make an independent test for systematic evolution in the distribution of SN luminosities.

Microscopic DM does not need to be clustered for this test to work. The clustering is added to make the calculations realistic. Clustering the microscopic DM to a greater or lesser extent would affect our results quantitatively, but the test would still be viable in more extreme cases. We conclude that if the

assumptions we have made about the noise levels in future SN observations remain reasonable, on the order of 50 – 100 SNe at $z \sim 1$ should suffice to determine a fundamental question: whether the major constituent of extragalactic DM is microscopic particles or macroscopic objects.

We would like to thank D. Holz for providing the results of his simulations for the purposes of comparison.

REFERENCES

Dyer C.C. & Roeder R.C., 1974, ApJ, 189, 167.

Garnavich, P.M. *et al.*, 1998, ApJ, 493, L53.

Holz D.E. & Wald, R.M., 1998, Phys. Rev. D, 58, 063501.

Kantowski R., 1998, ApJ, 507, 483.

Metcalf R.B., 1998a, MNRAS in press, astro-ph/9803319.

Metcalf R.B., 1998b, in “Evolution of Large-Scale Structure: From Recombination to Garching”, ed. Banday T., in press.

Metcalf R.B., 1999, in preparation.

Perlmutter S., *et al.*, 1997, ApJ, 483, 565.

Perlmutter S., *et al.*, 1998, Nature, 391, 51.

Premadi P., Martel H. & Matzner R., 1998, ApJ, 493, 10.

Riess A.G., Press W.H. & Kirshner R.P., 1996, ApJ, 473, 88.

Riess A.G. *et al.*, 1998, ApJ, 116, 1009.

Schneider P., Ehlers J. & Falco E.E., 1992, ‘Gravitational Lenses’, Springer-Verlag.

Schneider P. & Weiss A., 1988, ApJ, 327, 526.